Advanced Manufacturing and Characterization of mm-Wave Two-Layer Reflectarray Cells

Sam LeBlanc Department of Electrical Eng. and Computer Sci.

Embry-Riddle Aeronautical U. Daytona Beach, USA. leblans3@my.erau.edu Kenneth Church Sciperio Inc. Orlando, USA khc@sciperio.com

Eduardo Carrasco Information Processing and Telecommunications Center Univ. Politécnica de Madrid Madrid, Spain

© 0000-0002-4473-4095

Eduardo A. Rojas-Nastrucci Department of Electrical Eng. and Computer Sci. Embry-Riddle Aeronautical U. Daytona Beach, USA.

rojase1@erau.edu

Jose A. Encinar
Information Processing and
Telecommunications Center
Univ. Politécnica de Madrid
Madrid, Spain

00000-0002-2406-0847

Eduardo Martinez-de-Rioja Dept. of Signal Theory and Communications Universidad Rey Juan Carlos Madrid, Spain

Abstract— Reflectarray antennas (RA) have been proven as a transformational technology for a variety of applications, including space missions, where flat antenna reflectors are engineered with a great degree of freedom on operational bands and beam shapes. RA also offer the ability of using deployable flat geometries which are highly desirable for CubeSat missions. On the other hand, additive manufacturing processes have evolved over the last decade to achieve overall antenna performance and feature sizes that enable their operation for mm-wave frequencies. In this paper, dual-band RA elements are designed for the 18-32 GHz frequency band. The multilayer elements are fabricated using direct digital manufacturing, combining fused deposition modeling of polycarbonate (PC) and micro-dispensing of Ag ink, with an intermediate step of milling to enhance the surface roughness. The phase response of the elements is measured using WR-34 waveguides, and the geometry is inspected using X-Ray CT

Keywords— Additive Manufacturing, Reflectarray Antennas, WR-34 Waveguide.

I. INTRODUCTION

Over the last decade the reflectarray antennas (RA) have advanced, and its applications have been demonstrated in a variety of environments, including deployable antennas for space missions [1]. With the unique capability to achieve multiband operation and beam shaping over a flat surface, RA offer a great size and weight advantages over traditional parabolic reflectors. On the other hand, additive manufacturing (AM) has been demonstrated as a viable option to achieve high-performance antennas that are compatible with in-space manufacturing with unprecedented design degrees of freedom. Both technologies, RA design and AM, are combined in this paper to achieve mm-wave multilayer RA elements.

Reflectarray antennas are formed by a planar array of phasing cells, usually composed by conductive elements printed on single or multiple dielectric layers over a ground plane [2], illuminated by a primary feed. To achieve dual-band operation, reflectarray antennas based on a single layer (with different types of printed elements) [3]-[4] or stacked layers (one layer for each frequency) [5]-[7] have been proposed. Reflectarrays with phasing cells made of independent sets of parallel dipoles for each polarization printed on two layers have demonstrated very good performance to operate in dual frequency and dual linear polarization [6]. Multi-frequency reflectarrays at millimeterwave frequencies have many applications in communication systems, such as 5G networks or satellite communications.

AM has advanced to the point where it can provide an alternative to traditional printed circuit board (PCB) fabrication processes with an advantage of greater design freedom. Conductive traces and dielectric features can be accurately controlled and selectively placed to achieve geometries and performances that would otherwise not be possible [8]. Subtractive processes can be incorporated into AM to enhance its capabilities and performance such as increased conductivity and better surface finishes [9]-[10]. Furthermore, postprocessing techniques like in [9] can further increase performance. However, the direct manufacturing of multi-layer printed reflectarrays offers challenges to achieve dimensional accuracy for the dielectric layers and a pattern of conductive elements, as well as acceptable surface roughness to reduce the conductor losses. In this work, we demonstrate the direct additive manufacturing of reflectarray cells including two levels of conductive dipoles and a ground plane using a nScrypt system, with Polycarbonate (PC) as a dielectric, and HPS FG-77 silver conductive ink. 16-element three-conductive-layers reflectarray elements are achieved and characterized in the range 18-32 GHz.

II. DEFINITION OF REFLECTARRAY CELLS

The reflectarray cells considered in this work are similar to those used in [6] to design a dual-frequency reflectarray antenna for simultaneous operation at the 20 and 30 GHz bands. The cell is composed of two dielectric layers with two levels of printed dipoles, see Figs. 1(a) and 1(b). There are five parallel dipoles

This work is supported by the National Science Foundation under Grant 1944599, by the Spanish Ministry of Science and Innovation under Project PID2020-114172RB-C22C21-2/AEI/10.13039/501100011033 and by the European Regional Development Fund.

978-1-6654-2195-9/22/\$31.00 ©2022 IEEE

on the bottom layer, and three stacked dipoles on the upper layer. The dielectric material of both layers is Polycarbonate (PC), with relative permittivity $\varepsilon_r = 2.8$ and loss tangent $tan\delta = 0.0005$. The thickness of the lower PC layer is 1.3 mm, and the thickness of the upper PC layer is 0.6 mm. The lower dielectric layer is backed by the ground plane. The dimensions of the reflectarray cells are $L \times L$, where L = 4.318 mm. The width of the rectangular dipoles is 0.25 mm (same in both layers), and the distance between parallel dipoles is $S_A = 0.25$ mm for the lower layer and $S_B = 0.75$ mm for the upper layer (distances from edge to edge). The phase shift introduced at 20 GHz can be controlled by varying the lengths of the lower dipoles, while the lengths of the upper dipoles will adjust the phase shift at 30 GHz, as explained in [6].

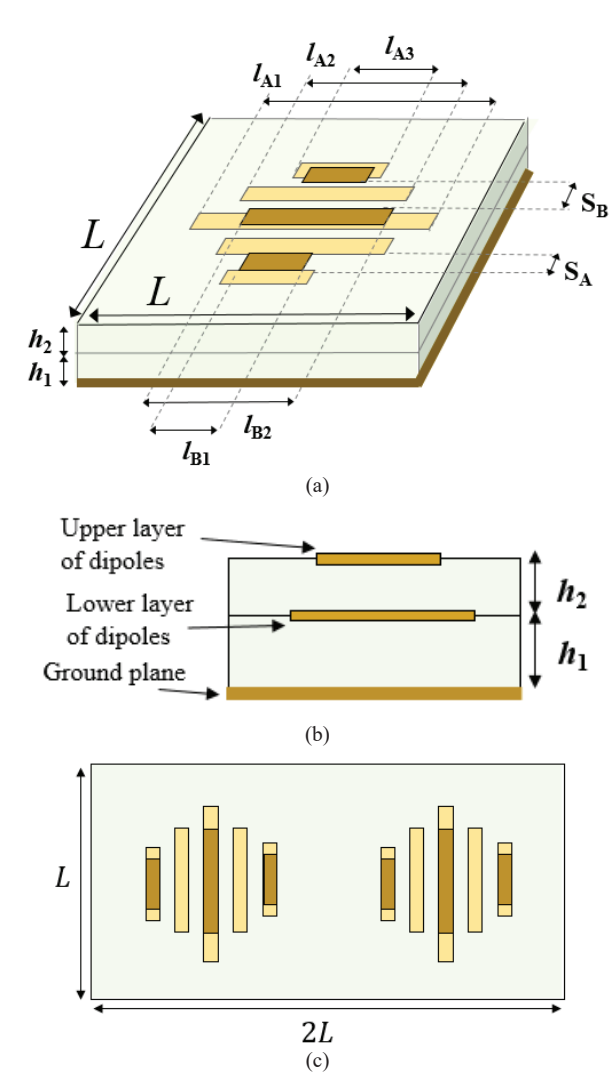


Fig. 1. (a) Perspective view of the reflectarray cell formed by stacked dipoles. (b) Lateral view with the stack configuration. (C) Upper view of the samples that will be manufactured and measured in a WGS, formed by two reflectarray cells.

Several samples containing the aforementioned reflectarray cells are manufactured and measured using the known technique of the rectangular waveguide simulator (WGS) [11]. The WR-34 waveguide (with dimensions of 4.318 mm x 8.636 mm) are used to confirm the performance of the reflectarray cell in the frequency band from 18 to 32 GHz. By the WGS method, the

dimensions of the samples must be equal to the opening of the waveguide. For this reason, the samples are formed by two contiguous reflectarray cells, as shown in Fig. 1(c). The metallic walls of the waveguide simulate a periodic environment for the cells, so the reflection coefficient of the manufactured samples is measured and compared with the electromagnetic simulations of the cell under the local periodicity assumption. To obtain a smooth phase variation in the 18-32 GHz band, the lengths of the dipoles have been adjusted to the following values: $I_{A1} = 3.9$ mm, $I_{A2} = 3.16$ mm, $I_{A3} = 2.42$ mm, $I_{B1} = 3.1$ mm, $I_{B2} = 2.51$ mm.

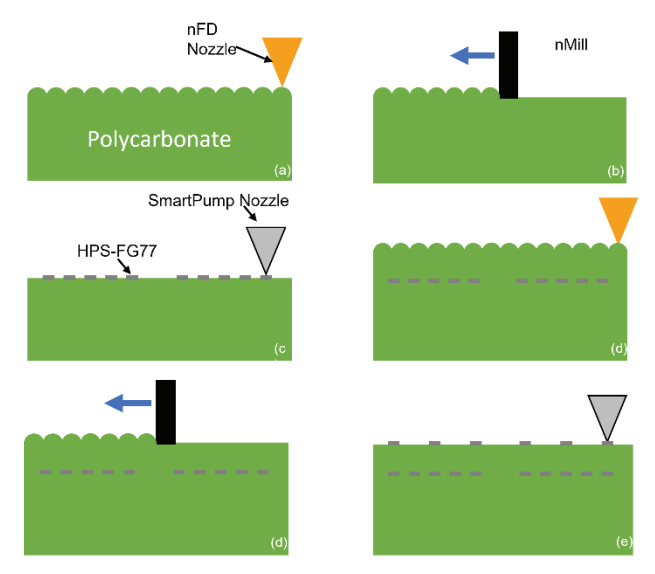


Fig. 2. Fabrication steps incorporating FFF 3D printing, micromachining, and microdispensing conductive paste.

III. ADDITIVE MANUFACTURING

The fabrication of the samples is performed in situ on an nScrypt 3Dn TableTop system, shown in Fig. 3. These systems combine multiple processes into a single machine. In this case, microdispensing, Fused Filament Fabrication (FFF) or 3D printing, and micromachining were all used to create these samples. To begin, the base PC layers are 3D printed with an nScrypt nFDTM 3D printing head using a 300 µm inner diameter nozzle with a layer height of 200 µm. The nozzle temperature is set to 350°C with a bed temperature of 100°C. Multiple layers are printed, using a specific infill direction (0°, 45°, or 90°) to a total thickness of 1.4mm, 100 µm greater than the desired 1.3 mm (Fig. 2 (a)). This is to account for the material that will be removed during the micromachining process. 3D printing can leave a relatively rough surface finish that is not conducive to microdispensing. "Hills" and "valleys" from the FFF process (Fig. 2 (a)) can interfere with microdispensed traces by causing material to wick away due to capillary forces, potentially causing shorts or other undesirable effects. Therefore, nScrypt's nMillTM milling head equipped with a 3mm diameter, 4-flute endmill with a speed of 5000 rpm and a feed rate of 50 mm/s, is used to remove 100µm of material, leaving a smooth surface with a roughness of less than 1 µm [9] (Fig. 2 (b)). This amount of material removal is chosen because it is equal to half the layer height of a single printed layer. This will result in the most densely filled surface since the cross section of a single printed line of material is circular. After the milling process, an nScrypt SmartPumpTM equipped with a 50 µm inner diameter nozzle is used to dispense NovaCentrixTM HPS-FG77 Ag nanoflake paste (Fig. 2 (c)). This conductive paste can reach ~3x bulk resistivity of copper after curing and performs exceptionally well for printing fine features due to its viscosity of 75000 cPs and average particle size of 0.3 μm. The material will dry on the substrate after printing due to the heated bed before the next layers of PC are printed. Once dried, the 3D printing process is repeated, embedding the dipoles into the PC. Once again, after the 3D printing process is complete, material is removed using the milling process, yielding a desirable surface finish. The top layer of dipoles is then microdispensed. Once this layer is dry, the entire sample is removed. The ground plane is then painted onto the bottom of the substrate using more HPS-FG77 and a small foam swab. The entire substrate is then put into an oven for a final cure at 120°C for 2 hours.

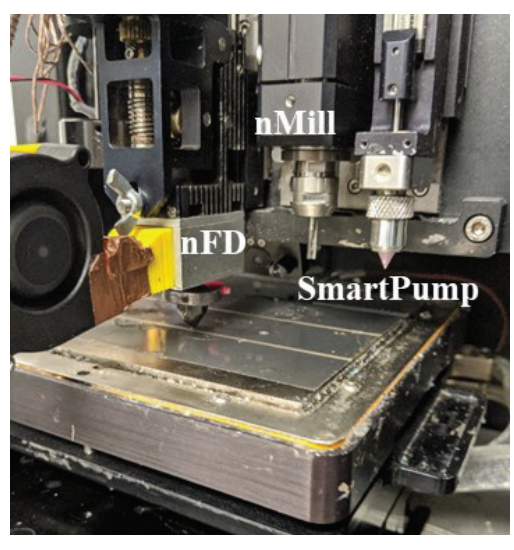


Fig. 3. Picture of the nScrypt 3Dn-TableTop system equipped with an nFD, nMill, and SmartPump.

IV. RESULTS

The fabricated samples with the reflectarray cells have been measured in a WGS in the frequency band from 18 to 32 GHz. The comparison between the simulated and measured phase of the reflection coefficient versus frequency is presented in Fig. 4(a). As can be seen, the phase of the reflection coefficient presents several resonances and a reasonable agreement with the simulated response. Three resonances are clearly identified on the measured curves of the reflection coefficient amplitude (Fig. 4(b)), with very high values of losses. However, the simulated losses of the reflectarray cell (also shown in the figure) are lower than 0.5 dB. The higher losses measured can be attributed to a poor electric contact of the ground plane inside the waveguide. We are working to modify the measurements set-up to avoid this problem.

A KeyenceTM VKx-3000 laser confocal microscope was used to image the top of the sample (Fig. 5). A SkyScan1275TM was used to perform an X-Ray CT scan to measure the internal features of the printed reflectarray sample as shown in Fig. 6, while the internal features measured are as follows: $l_{A1} = 3.652$ mm, $l_{A2} = 3.05$ mm, $l_{A3} = 2.504$ mm, $l_{B1} = 3.02$ mm, $l_{B2} = 2.499$ mm, and the width varied from 0.211 mm - 0.226 mm. The layer thicknesses measured $h_1 = 1.254$ mm and $h_2 = 0.674$

mm for an overall thickness of 1.928 mm. The errors in the dipole lengths (< 0.25 mm) and substrate thickness (< 0.08 mm) have produced a slight variation of the phase curves as shown in Fig. 4(a).

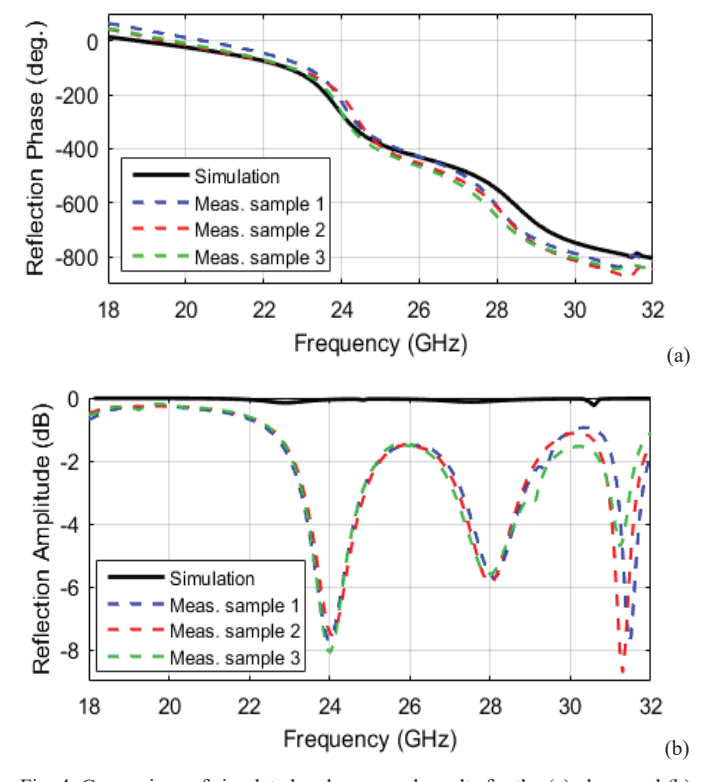


Fig. 4. Comparison of simulated and measured results for the (a) phase and (b) amplitude of the reflection coefficient versus frequency.

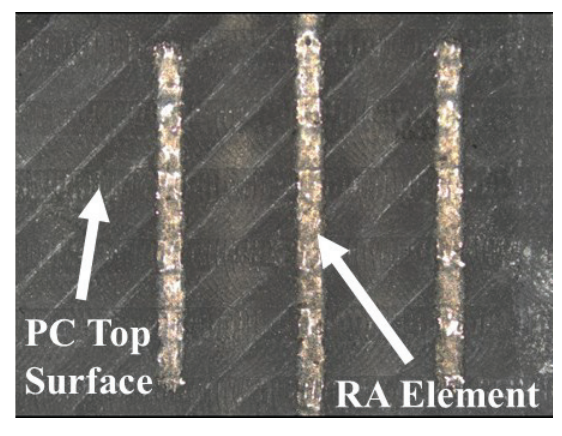


Fig. 5. Micrograph of the manufactured elements of the reflectarray.

V. CONCLUSIONS

The advanced manufacturing of two-layer mm-wave reflectarray cells, including additive manufacturing of the dielectric and conductive layers, has been demonstrated. Several samples have been designed, manufactured, and tested in a waveguide simulator, to validate the electrical characterization of the reflectarray cells. The measured results show good agreement with simulations and an acceptable phase response with three resonances. The high losses at the resonances is caused by the test setup. These reflectarray cells will be used for direct manufacturing of a full reflectarray operating in two

frequency bands. Future work include adjustment of the manufacturing process to achieve dimensions that are closer to the ideal design values, as well as improving the measurement process to reduce losses due to poor contact between the cell ground plane and the end of the waveguide section.

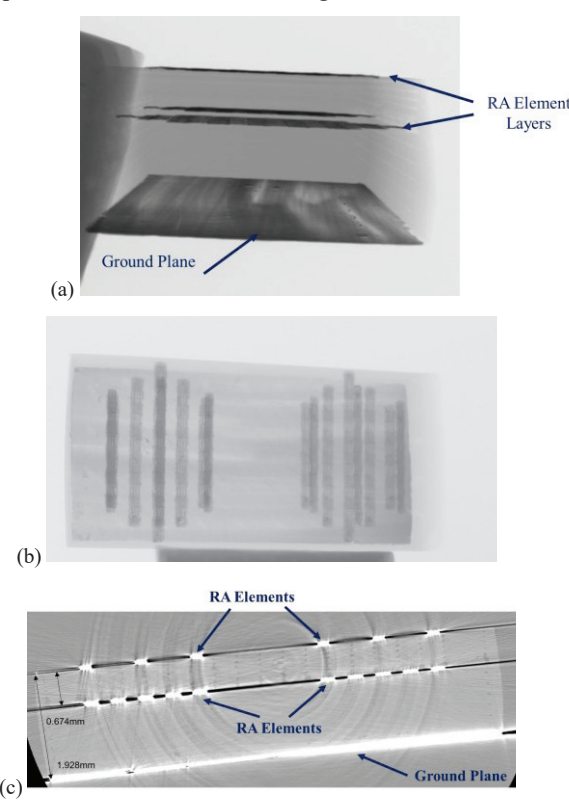


Fig. 6. X-Ray CT scan of printed reflectarray samples. (a) Side-view showing surface dipoles, embedded dipoles, and ground plane, (b) top view, and (c) cross-sectional view.

REFERENCES

- [1] Noemi Miguélez-Gómez, et al., "Thickness-Accomodation in X-Band Origami-based Reflectarray Antenna for Small Satellites Applications," IEEE International Conference on Wireless for Space and Extreme Environments (WiSEE), Vicenza, Italy, 2020.
- [2] J. Huang and J. A. Encinar, "Reflectarray Antennas", IEEE Press/Wiley, Piscataway, New Jersey, 2008.
- [3] R. Deng, Y. Mao, S. Xu, and F. Yang, "A single-layer dual-band circularly polarized reflectarray with high aperture efficiency," IEEE Trans. Antennas Propagat., vol. 63, no.7, pp. 3317–3320, Jul. 2015.
- [4] T. Smith, U. V. Gothelf, O. S. Kim, and O. Breinbjerg, "Design, manufacturing, and testing of a 20/30 GHz dual-band circularly polarized reflectarray antenna in submission," IEEE Antennas Wireless Propag. Lett., vol. 12, pp. 1480–1483, 2013.
- [5] E. Martinez-de-Rioja, J. A. Encinar, M. Barba, R. Florencio, R. R. Boix, V. Losada, "Dual polarized reflectarray transmit antenna for operation in Ku- and Ka-bands with independent feeds", IEEE Trans. Antennas Propag., vol. 65, no. 6, pp. 3241–3246, Jun. 2017.
- [6] E. Martinez-de-Rioja, J. A. Encinar, R. Florencio, R. R. Boix, "Reflectarray in K and Ka bands with independent beams in each polarization", Proc. 2016 IEEE International Symposium on Antennas and Propagation (APSURSI), Fajardo, PR, USA, 2016, pp. 1150–1199.
- [7] E. Martinez-de-Rioja, D. Martinez-de-Rioja, R. Lopez-Saez, I. Linares, J. A. Encinar, "High-Efficiency Polarizer Reflectarray Antennas for Data Transmission Links from a CubeSat", Electronics, MDPI, vol. 10, 1082, 2021.
- [8] T. P. Ketterl et al., "A 2.45 GHz Phased Array Antenna Unit Cell Fabricated Using 3-D Multi-Layer Direct Digital Manufacturing," in *IEEE Transactions on Microwave Theory and Techniques*, vol. 63, no. 12, pp. 4382-4394, Dec. 2015
- [9] E. A. Rojas-Nastrucci et al., "Characterization and Modeling of K-Band Coplanar Waveguides Digitally Manufactured Using Pulsed Picosecond Laser Machining of Thick-Film Conductive Paste," in *IEEE Transactions* on Microwave Theory and Techniques, vol. 65, no. 9, pp. 3180-3187, Sept. 2017
- [10] S. LeBlanc, K. Church and E. A. Rojas-Nastrucci, "Photonic Curing of mm-Wave Coplanar Waveguides for Conductor Loss Enhancement," 2021 IEEE 21st Annual Wireless and Microwave Technology Conference (WAMICON), 2021,
- [11] P. W. Hannan and M. A. Balfour, "Simulation of a phased-array antenna in waveguide", IEEE Trans. Antennas Propag., vol. 13, no. 3, pp. 342– 353, May 1965.